Towards the optical second: verifying optical clocks at the SI limit

W. F. McGrew,[1,2] X. Zhang,[1] H. Leopardi,[1,2] R. J. Fasano,[1,2] D. Nicolodi,[1,2] K. Beloy,[1] J. Yao,[1,2] J. A. Sherman,[1] S. A. Schäffer,[1,3] J. Savory,[1] R. C. Brown,[1,4] S. Römisch,[1] C. W. Oates,[1] T. E. Parker,[1,5] T. M. Fortier,[1,6] and A. D. Ludlow[1,2,7]

[1]*National Institute of Standards and Technology, 325 Broadway, Boulder, Colorado 80305, USA*
[2]*Department of Physics, University of Colorado, Boulder, Colorado 80309, USA*
[3]*Niels Bohr Institute, University of Copenhagen, Blegdamsvej 17, 2100 Copenhagen, Denmark*
[4]*Present address: Georgia Tech Research Institute, Atlanta, Georgia 30332, USA*
[5]*e-mail: tom.parker@nist.gov*
[6]*e-mail: tara.fortier@nist.gov*
[7]*e-mail: andrew.ludlow@nist.gov*

The pursuit of ever more precise measures of time and frequency motivates redefinition of the second in terms of an optical atomic transition. To ensure continuity with the current definition, based on the microwave hyperfine transition in ^{133}Cs, it is necessary to measure the absolute frequency of candidate optical standards relative to primary cesium references. Armed with independent measurements, a stringent test of optical clocks can be made by comparing ratios of absolute frequency measurements against optical frequency ratios measured via direct optical comparison. Here we measure the $^1S_0 \rightarrow \, ^3P_0$ transition of ^{171}Yb using satellite time and frequency transfer to compare the clock frequency to an international collection of national primary and secondary frequency standards. Our measurements consist of 79 runs spanning eight months, yielding the absolute frequency to be 518 295 836 590 863.71(11) Hz and corresponding to a fractional uncertainty of 2.1×10^{-16}. This absolute frequency measurement, the most accurate reported for any transition, allows us to close the Cs-Yb-Sr-Cs frequency measurement loop at an uncertainty $<3 \times 10^{-16}$, limited for the first time by the current realization of the second in the International System of Units (SI). Doing so represents a key step towards an optical definition of the SI second, as well as future optical time scales and applications. Furthermore, these high accuracy measurements distributed over eight months are analyzed to tighten the constraints on variation of the electron-to-proton mass ratio, $\mu = m_e/m_p$. Taken together with past Yb and Sr absolute frequency measurements, we infer new bounds on the coupling coefficient to gravitational potential of $k_\mu = (-1.9 \pm 9.4) \times 10^{-7}$ and a drift with respect to time of $\frac{\dot{\mu}}{\mu} = (5.3 \pm 6.5) \times 10^{-17}/\text{yr}$.   © 2019 Optical Society of America under the terms of the [OSA Open Access Publishing Agreement](#)

https://doi.org/10.1364/OPTICA.6.000448

1. INTRODUCTION

Since the first observation of the 9.2 GHz hyperfine transition of ^{133}Cs, it was speculated that atomic clocks could outperform any conventional frequency reference, due to their much higher oscillation frequency and the fundamental indistinguishability of atoms [1]. Indeed, Harold Lyons' 1952 prediction that "an accuracy of one part in ten billion may be achieved" has been surpassed one million-fold by atomic fountain clocks with systematic uncertainties of a few parts in 10^{16} [2]. The precision of atomic frequency measurements motivated the 1967 redefinition of the second in the International System of Units (SI), making time the first quantity to be based upon the principles of nature, rather than upon a physical artifact [3]. The superior performance of atomic clocks has found numerous applications, most

notably enabling global navigation satellite systems (GNSS), where atomic clocks ensure precise time delay measurements that can be transformed into position measurements [4].

Microwave atomic fountain clocks exhibit a quality factor on the order of 10^{10}, and the current generation can determine the line center at 10^{-6} of the linewidth. This, along with a careful accounting of all systematic biases, leads to an uncertainty of several parts in 10^{16}, i.e., the SI limit. Significant improvement of microwave standards is considered unrealistic; however, progress has been realized utilizing optical transitions, where the higher quality factor of approximately 10^{15} allows many orders of magnitude improvement [5,6]. For example, a recent demonstration of two ytterbium optical lattice clocks at the National Institute of Standards and Technology (NIST) found instability, systematic

uncertainty, and reproducibility at the 1×10^{-18} level or better, thus outperforming the current realization of the second by a factor of >100 [7]. The superior performance of optical clocks motivates current exploratory work aimed at incorporating optical frequency standards into existing time scales [8–13]. Furthermore, for the first time, the gravitational sensitivity of these clocks surpasses state-of-the-art geodetic techniques and promises to find application in the nascent field of chronometric leveling [14]. Optical frequency references could potentially be standards not only of time, but of space-time.

Towards the goal of the eventual redefinition of the SI unit of time based on an optical atomic transition, the International Committee for Weights and Measures (CIPM) in 2006 defined secondary representations of the second so that other transitions could contribute to the realization of the SI second, albeit with an uncertainty limited at or above that of cesium (Cs) standards [15]. Optical transitions designated as secondary representations (eight at the time of this writing) represent viable candidates for a future redefinition to an optical second, and the CIPM has established milestones that must be accomplished before adopting a redefinition [16]. Two key milestones are absolute frequency measurements limited by the $\approx 10^{-16}$ performance of Cs, in order to ensure continuity between the present and new definitions, and frequency ratio measurements between different optical standards, with uncertainty significantly better than 10^{-16}. These two milestones together enable a key consistency check: it should be possible to compare a frequency ratio derived from absolute frequency measurements to an optically measured ratio with an inaccuracy limited by the systematic uncertainty of state-of-the-art Cs fountain clocks. Here we present a measurement of the ^{171}Yb absolute frequency that allows a "loop closure" consistent with zero at 2.4×10^{-16}, i.e., at an uncertainty that reaches the limit given by the current realization of the SI second.

2. EXPERIMENTAL SCHEME

This work makes use of the 578 nm $^1S_0 \rightarrow {}^3P_0$ transition of neutral ^{171}Yb atoms trapped in the Lamb–Dicke regime of an optical lattice at the operational magic wavelength [17,18]. The atomic system is identical to that described in Ref. [7] and has a systematic uncertainty of 1.4×10^{-18}. We note that only two effects (blackbody radiation shift and second-order Zeeman effect) could affect the measured transition frequency at a level that is relevant for the 10^{-16} uncertainties of the present measurement. Several improvements have reduced the need to optimize experimental operation by reducing the need for human intervention. A digital acquisition system is used to monitor several experimental parameters. If any of these leaves the nominal range, data are automatically flagged to be discarded in data processing. An algorithm for automatically reacquiring the frequency lock for the lattice laser was employed. With these improvements, an average uptime of 75% per run was obtained during the course of 79 separate runs of average duration of 4.9 h, distributed over eight months (November 2017 to June 2018).

The experimental setup is displayed in Fig. 1. A quantum-dot laser at 1156 nm is frequency-doubled and used to excite the 578 nm clock transition in a spin-polarized, sideband-cooled atomic ensemble trapped in an optical lattice. Laser light resonant with the dipole-allowed $^1S_0 \rightarrow {}^1P_1$ transition at 399 nm is used to destructively detect atomic population, and this signal is integrated to apply corrections of the 1156 nm laser frequency so as to stay resonant with the ultranarrow clock line. Some of this atom-stabilized 1156 nm light is sent, via a phase-noise-canceled optical fiber, to an octave-spanning, self-referenced Ti:sapphire frequency comb [19,20], where the optical frequency is divided down to $f_{rep} = 1$ GHz $- \Delta$. This microwave frequency is mixed with a hydrogen maser (labeled here ST15), multiplied to a nominal 1 GHz, and the resultant $\Delta \approx 300$ kHz heterodyne beat note is counted.
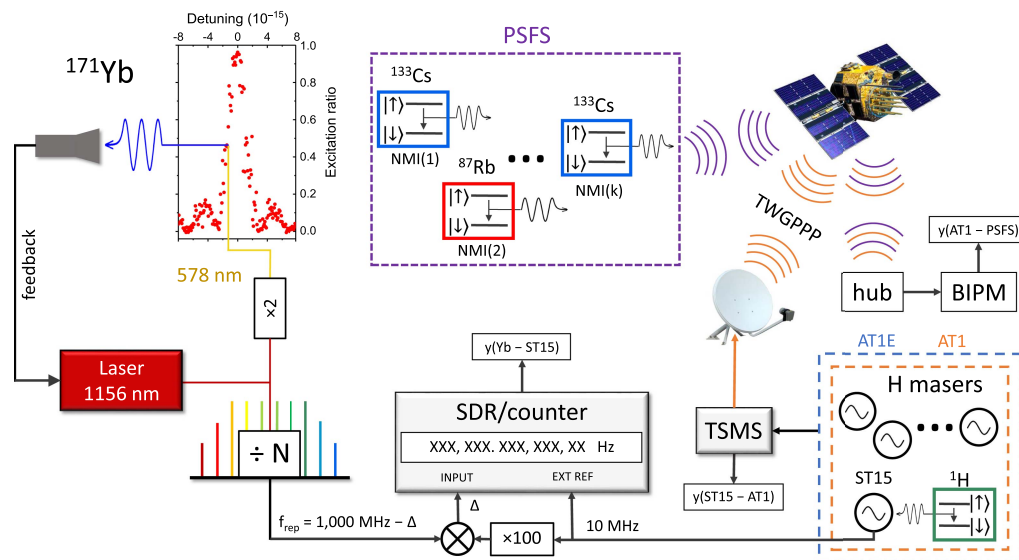

Fig. 1. Experimental setup of the Yb optical lattice standard. A counter or SDR measures the beat note between f_{rep} and the nominal 1 GHz reference derived from hydrogen maser ST15. The frequency of ST15 is compared by the NIST TSMS to that of two maser time scales—AT1E (blue) and AT1 (orange); see Supplement 1. These time scales utilize the same masers (approximately eight, including ST15) but differ in the statistical weight given to each maser [21]. The frequency of AT1 is sent to a central hub (the "star topology" used in TAI computations) via the TWGPPP protocol [22]. The measurements are then sent from the hub to the BIPM by an internet connection, and the BIPM publishes data allowing a comparison of AT1 against PSFS, composed of k separate clocks in different National Metrological Institutes (NMIs), where k varies from five to eight during the measurements.

The act of dividing the optical frequency down to 1 GHz may introduce systematic errors. Optical frequency synthesis introduces uncertainty that has been assessed through optical-optical comparisons to be well below 10^{-19}, insignificant for the present experiment [23,24]. However, for the present optical-microwave comparison, technical sources of error arising from the microwave setup may lead to inaccuracy greater by orders of magnitude. The nominal 10 MHz maser signal is multiplied by 100, to 1 GHz, by means of a frequency multiplier based on a phase-locked-loop. Electronic synthesis uncertainty is assessed by homodyne detection of the maser signal mixed with a 10 MHz signal generated by a direct digital synthesizer referenced to the 1 GHz signal. Electronic synthesis is found to contribute errors no larger than 3×10^{-17}. Another source of uncertainty arises from counting error. The first half of the data set is obtained using a 10-second-gated commercial frequency counter to count the heterodyne beat note. Counting error is assessed by measuring the 10 MHz maser signal, also used as the counter's external reference. This counting error contributes an uncertainty of as much as 6×10^{-14} of Δ, leading to an error of $<2 \times 10^{-17}$ on f_{rep}, and thus also on the optical frequency. The second half of the data set is obtained by replacing the counter with a software-defined radio (SDR) in two-channel differential mode [25]. The SDR phase continuously measured the frequency once per second with zero dead time. The hardware acquisition rate and effective (software digital filter) noise bandwidth were 1 MHz and 50 Hz, respectively. For all run durations the counting error of the SDR is $<1 \times 10^{-17}$ of f_{rep}.

After the optical signal is downconverted and compared to the hydrogen maser ST15, the comb equation is used to determine a normalized frequency difference between the Yb optical standard and the maser, y(Yb-ST15). Throughout this work, we express normalized frequency differences between frequency standards A and B as follows:

$$y(A - B) \equiv y_A(t) - y_B(t) = \frac{\nu_A^{\text{act}}}{\nu_A^{\text{nom}}} - \frac{\nu_B^{\text{act}}}{\nu_B^{\text{nom}}} \approx \frac{\nu_A^{\text{act}}/\nu_B^{\text{act}}}{\nu_A^{\text{nom}}/\nu_B^{\text{nom}}} - 1, \quad (1)$$

where $\nu_X^{\text{act(nom)}}$ is the actual (nominal) frequency of standard X, and the approximation is valid in the limit $(\nu_X^{\text{act}} - \nu_X^{\text{nom}})/\nu_X^{\text{nom}} \ll 1$, a well-founded assumption throughout this work. In the definition of y(Yb-ST15), $\nu_{\text{Yb}}^{\text{nom}} = \nu_{\text{Yb}}^{\text{CIPM17}} = 518\,295\,836\,590\,863.6$ Hz is the 2017 CIPM recommended frequency of the Yb clock transition [16] and $\nu_{\text{ST15}}^{\text{nom}} = 10$ MHz. The NIST time scale measurement system (TSMS) is used to transfer the frequency difference, y(Yb-ST15), from maser ST15 to a local maser time scale, labeled AT1E, which is significantly stabler than ST15. The time scale serves as a flywheel oscillator for a comparison to an average of primary and secondary frequency standards (PSFS), which the International Bureau of Weights and Measures (BIPM) publishes with a resolution of one month in Circular T [26]. The dead time uncertainty [27] associated with intermittent operation of the optical standard is comprehensively evaluated in Part A of Supplement 1 and amounts to the largest source of statistical uncertainty; see Table 1. The maser time scale frequency is transmitted to the BIPM via the hybrid Two-Way Satellite Time and Frequency Transfer/GPS Precise Point Positioning (TWGPPP) frequency transfer protocol [22], and the frequency transfer uncertainty is the second largest source of statistical uncertainty. The transfer process from the local maser time scale to PSFS is described in

Table 1.   Uncertainty Budget of the Eight-Month Campaign for the Absolute Frequency Measurement of the ^{171}Yb Clock Transition

Uncertainty (10^{-16})	March 2018[a]	Full Campaign
Type A uncertainty		
Dead time	2.5	1.0
Frequency transfer	2.6	0.9
Yb-maser comparison	0.8	0.4
Time scale measurement	<0.1	<0.1
PSFS	1.4	0.5
Total type A	**4.0**	**1.6**
Frequency comb type B uncertainty		
Optical synthesis	<0.001	<0.001
Electronic synthesis	0.3	0.3
Counter/SDR	0.1	0.1
Total comb type B	**0.3**	**0.3**
PSFS type B	**1.4**	**1.3**
Yb type B	**0.014**	**0.014**
Relativistic redshift	**0.06**	**0.06**
Total	**4.2**	**2.1**

[a]Data for March 2018 are shown as an example of one month's data.

Part B of Supplement 1. The frequency transfer processes from ST15 to the local maser time scale and finally to PSFS are continuously operating, thus transferring the frequencies between the standards with no dead time. However, the comparison data are published by the BIPM on a grid roughly corresponding to a month (with duration of 25, 30, or 35 days).

3. RESULTS AND ANALYSIS

We made 79 measurements over the course of eight months, for a total measurement interval of 12.1 days, or a 4.9% effective duty cycle. The weighted mean of the eight monthly values, y_{m}(Yb-PSFS), gives a value for the total normalized frequency difference obtained from these measurements, y_{T}(Yb-PSFS) and its associated uncertainty. The statistical (type A) and systematic (type B) uncertainties are accounted for in Table 1. Type B uncertainties tend to be highly correlated over time and therefore do not average down with further measurement time. For the uncertainty budgets of state-of-the-art Cs fountain clocks, the leading term is locally determined (e.g., microwave-related effects or density effects). Following convention, here we treat the type B uncertainties of the PSFS ensemble's constituent fountain clocks [28–33] as uncorrelated between standards, leading to a PSFS type B uncertainty of 1.3×10^{-16}, lower than the uncertainty of any individual fountain. We measure a value of $\nu_{\text{Yb}} = 518295836590863.71(11)$ Hz. The difference between our measurement and the CIPM recommended value is $(2.1 \pm 2.1) \times 10^{-16}$, where the stated error bar corresponds to the 1σ uncertainty of the mean value. This should be compared to the CIPM's recommended uncertainty estimation of 5×10^{-16} [16]. The reduced chi-squared statistic, χ_{red}^2, is 0.98, indicating that the scatter in the eight monthly values is consistent with the stated uncertainties. This represents the most accurate absolute frequency measurement yet performed on any transition. Furthermore, good agreement is found between this measurement and previous absolute frequency measurements of the Yb transition (Fig. 2). If a line is fit to our data, the slope is found
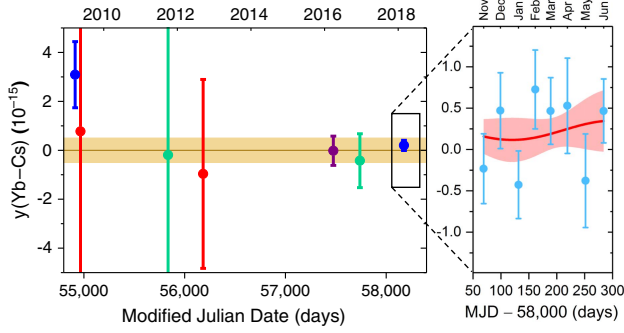
Fig. 2. Absolute frequency measurements of the $^1S_0 \rightarrow {}^3P_0$ transition frequency measured by four different laboratories: NIST (blue) [18], National Metrological Institute of Japan (red) [34,35], the Korea Research Institute of Standards and Science (green) [36,37], and the Istituto Nazionale di Ricerca Metrologica (purple) [38]. The light-blue points in the inset represent the eight monthly values reported in this work, y_m(Yb-PSFS), and the final dark blue point represents y_T(Yb-PSFS). The yellow shaded region represents the 2017 CIPM recommended frequency and uncertainty. The inset shows a sinusoidal fit of the coupling parameter to gravitational potential for measurements of the frequency ratio between Yb and Cs between November 2017 and June 2018. The red shaded region in the inset represents 1σ uncertainty in the fit function.

to be $(2.0 \pm 2.2) \times 10^{-18}$/day, indicating that there is no statistically significant frequency drift.

Due to the unavailability of a local Cs primary frequency reference during this period, these measurements were performed without one. This mode of operation limits the achievable instability—with a local Cs fountain clock and a low-instability microwave oscillator, it is possible to achieve type A uncertainties at the low 10^{-16} level after one day of averaging, whereas in our configuration this was not achieved until >10 days of cumulative run time. Furthermore, it is necessary to correctly account for dead time uncertainty, as frequency measurements of the maser time scale against PSFS are published on a very coarse grid. On the other hand, the unprecedented accuracy reported in this work is directly facilitated by the lower type B uncertainty associated with the PSFS ensemble, as compared with any single Cs

fountain. An additional advantage to this mode of operation is that it is straightforward to determine frequency ratios with other secondary representations of the second that may be contributing to PSFS. For example, during these measurements, a Rb fountain clock (SYRTE FORb) contributed to PSFS [31], allowing the first direct measurement of the Yb/Rb ratio, found to be $\nu_{Yb}/\nu_{Rb} = 75\,833.197\,545\,114\,192\,(33)$; see Part C of Supplement 1.

It is desirable to establish the consistency of frequency ratios determined through direct comparisons and through absolute frequency measurements. For absolute frequencies, the CIPM recommended values are based upon a least-squares algorithm that takes as inputs both absolute frequency measurements, as well as optical ratio measurements [16,39]. To establish the consistency between absolute frequency measurements and direct optical ratio measurements, we determine average frequencies only from the former, as a weighted average of all previous measurements. If $\chi^2_{red} > 1$, we expand the uncertainty of the mean by $\sqrt{\chi^2_{red}}$. For the Yb frequency, we determine a weighted average of the present work and six previous measurements [18,34–38], $\nu_{Yb}^{avg} = 518\,295\,836\,590\,863.714\,(98)$ Hz, with $\chi^2_{red} = 0.85$. For the Sr frequency, we likewise determine a weighted average of 17 previous measurements [9,10,40–54], $\nu_{Sr}^{avg} = 429\,228\,004\,229\,873.055\,(58)$ Hz, with $\chi^2_{red} = 0.57$. The frequency ratio derived from absolute frequency measurements is, therefore, $\mathcal{R}_{abs}^{avg} = \nu_{Yb}^{avg}/\nu_{Sr}^{avg} = 1.207\,507\,039\,343\,337\,86\,(28)$. A frequency ratio can also be determined directly from optical frequency ratio measurements. From a weighted average of six optical ratio measurements [55–60], we determine $\mathcal{R}_{opt}^{avg} = 1.207\,507\,039\,343\,337\,768\,(60)$, with $\chi^2_{red} = 1.28$. All three averages exhibit a χ^2_{red} close to 1, indicating that the scatter is mostly consistent with the stated uncertainties; only the uncertainty of optical ratios is rescaled, and that only modestly. We therefore determine a loop misclosure of $(\mathcal{R}_{abs} - \mathcal{R}_{opt})/\mathcal{R} = (0.8 \pm 2.4) \times 10^{-16}$, indicating consistency between the optical and microwave scales at a level that is limited only by the uncertainties of Cs clocks. This agreement is demonstrated graphically in Fig. 3. We emphasize that each of the three legs of the loop—Yb absolute frequency, Sr absolute frequency, and
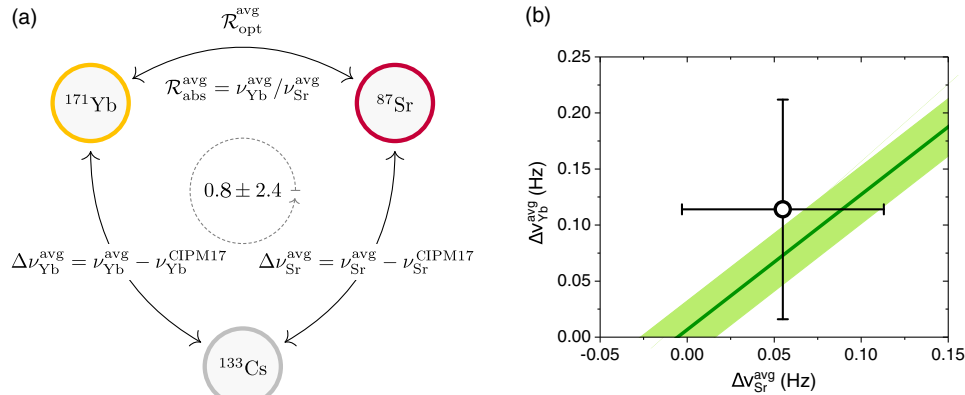

Fig. 3. Graphical representation of the agreement between frequency ratios derived from absolute frequency measurements of ^{171}Yb and ^{87}Sr and direct optical measurements. (a) Schematic of the Cs-Yb-Sr-Cs loop that is examined. The central number is the misclosure, as parts in 10^{16}. (b) Average Yb and Sr frequency, offset from the CIPM 2017 recommended values, parametrically plotted against each other. The error bars are the 1σ uncertainty in the averaged absolute frequency measurements. The optical ratio measurement (dark green) appears as a line in this parameter-space, with the shaded region representing the uncertainty of the ratio. Frequency ratios derived from absolute frequencies agree well with ratios measured optically.

Table 2.   Measurements of Coupling of Dimensionless Constants to Gravitational Potential, with Sensitivity Coefficients, ΔK, from [62–64]

No.	Reference	X, Y	$\beta_{X,Y}(10^{-6})$	$\Delta K_{X,Y}^{\alpha}$	$\Delta K_{X,Y}^{X_q}$	$\Delta K_{X,Y}^{\mu}$
(i)	Dzuba & Flambaum, 2017 [65]	Al^+, Hg^+	0.16 ± 0.30	2.95	0	0
(ii)	Ashby *et al.*, 2018 [66]	H, Cs	0.22 ± 0.25	−0.83	−0.102	0
(iii)	This work	Yb, Cs	-0.8 ± 1.4	−2.52	−0.002	−1

Yb/Sr ratio—feature different measurements performed at multiple laboratories across the world and are thus largely uncorrelated to each other.

4. NEW LIMITS ON COUPLING OF m_e/m_p TO GRAVITATIONAL POTENTIAL

Many beyond-Standard-Model theories require that parameters traditionally considered fundamental constants may vary across time and space [61]. This hypothesized variation is detectable by looking for a change in the frequency ratio of two different types of atomic clock [62]. We analyze our eight-month frequency comparison data to place bounds upon a possible coupling of the measured Yb/Cs frequency ratio to the gravitational potential of the Sun. We fit our data to y(Yb-PSFS) = $A \cos(2\pi(t - t_0)/1 \text{ yr}) + y_0$, where A and y_0 are free parameters, t is the median date for each of the eight months, t_0 is the date of the 2018 perihelion, and 1 yr = 365.26 days is the mean length of the anomalistic year. From our data, we determine the yearly variation of the Yb/Cs ratio, $A_{\text{Yb,Cs}} = (-1.3 \pm 2.3) \times 10^{-16}$; see the inset to Fig. 2. The amplitude of the annual variation of the gravitational potential is $\Delta\Phi = (\Phi_{\text{max}} - \Phi_{\text{min}})/2 \approx (1.65 \times 10^{-10})c^2$, where c is the speed of light in vacuum. Therefore, the coupling of the Yb/Cs ratio to gravitational potential is given by $\beta_{\text{Yb,Cs}} = A_{\text{Yb,Cs}}/(\Delta\Phi/c^2) = (-0.8 \pm 1.4) \times 10^{-6}$. A nonzero β coefficient would indicate a violation of the Einstein equivalence principle, which requires that the outcome of any local experiment (e.g., a frequency ratio measurement) is independent of the location at which the experiment was performed. Here we did not observe any violation of the equivalence principle.

Were this violation to occur, it might arise due to variation of the fine structure constant, α; the ratio of the light quark mass to the quantum chromodynamics (QCD) scale, $X_q = m_q/\Lambda_{\text{QCD}}$; or the electron-to-proton mass ratio, $\mu = m_e/m_p$. To discriminate among each of these constants, we combine our results with two previous measurements—an analysis [65] of a prior optical-optical measurement [67] and a microwave-microwave measurement [66]. These results are chosen as they exhibit sensitivities to fundamental constants that are nearly orthogonal to each other and to our optical-microwave measurement. Table 2 displays the coupling to gravitational potential observed in each measurement, as well as the differential sensitivity parameter $\Delta K_{X,Y}^{\epsilon}$, defined by $\delta y(X - Y) = \sum_{\epsilon} \Delta K_{X,Y}^{\epsilon}(\delta\epsilon/\epsilon)$, where X and Y are the two atomic clocks being compared, and ϵ is α, X_q, or μ. Values of $\Delta K_{X,Y}^{\epsilon}$ are from [62–64]. Rescaling the β parameter to sensitivity yields a parameter quantifying coupling to gravity potential, $k_{\epsilon} = \beta_{X,Y}/\Delta K_{X,Y}^{\epsilon}$. We first use line (i) of Table 2 to constrain the coupling parameter of α, $k_{\alpha} = (0.5 \pm 1.0) \times 10^{-7}$. Applying this coefficient to line (ii) and propagating the errors, we find $k_{X_q} = (-2.6 \pm 2.6) \times 10^{-6}$. Applying both of these coefficients to the present work in line (iii), we obtain a coupling coefficient to gravitational potential of $k_{\mu} = (0.7 \pm 1.4) \times 10^{-6}$. This value

represents an almost fourfold improvement over the previous constraint, $k_{\mu} = (-2.5 \pm 5.4) \times 10^{-6}$ [68]. In Part D of Supplement 1, we extend our analysis to the full record of all Yb and Sr absolute frequency measurements to infer $k_{\mu} = (-1.9 \pm 9.4) \times 10^{-7}$ and $\frac{\dot{\mu}}{\mu} = (5.3 \pm 6.5) \times 10^{-17}$/yr.

5. CONCLUSIONS

We have presented the most accurate spectroscopic measurement of any optical atomic transition, i.e., with the lowest uncertainty with respect to the SI realization of the second. We find that the frequency ratio derived from ^{171}Yb and ^{87}Sr absolute frequency measurements agrees with the optically measured ratio at a level that is primarily limited by the uncertainties of state-of-the-art fountain clocks. This level of agreement bolsters the case for redefinition in terms of an optical second. Further progress can be realized by the closing of loops consisting exclusively of optical clocks, since the improved precision of these measurements will allow misclosures that are orders of magnitude below the SI limit.

REFERENCES

1. H. Lyons, "Spectral lines as frequency standards," Ann. N.Y. Acad. Sci. **55**, 831–871 (1952).
2. T. P. Heavner, E. A. Donley, F. Levi, G. Costanzo, T. E. Parker, J. H. Shirley, N. Ashby, S. Barlow, and S. R. Jefferts, "First accuracy evaluation of NIST-F2," Metrologia **51**, 174–182 (2014).
3. J. Terrien, "News from the International Bureau of Weights and Measures," Metrologia **4**, 41–45 (1968).
4. N. Ashby, "Relativity and the global positioning system," Phys. Today **55**(5), 41–47 (2002).
5. J. L. Hall, "Nobel lecture: defining and measuring optical frequencies," Rev. Mod. Phys. **78**, 1279–1295 (2006).
6. A. D. Ludlow, M. M. Boyd, J. Ye, E. Peik, and P. O. Schmidt, "Optical atomic clocks," Rev. Mod. Phys. **87**, 637–701 (2015).
7. W. F. McGrew, X. Zhang, R. J. Fasano, S. A. Schäffer, K. Beloy, D. Nicolodi, R. C. Brown, N. Hinkley, G. Milani, M. Schioppa, T. H. Yoon, and A. D. Ludlow, "Atomic clock performance enabling geodesy below the centimetre level," Nature **564**, 87–90 (2018).
8. T. Ido, H. Hachisu, F. Nakagawa, and Y. Hanado, "Rapid evaluation of time scale using an optical clock," J. Phys. Conf. Ser. **723**, 012041 (2016).

9. C. Grebing, A. Al-Masoudi, S. Dörscher, S. Häfner, V. Gerginov, S. Weyers, B. Lipphardt, F. Riehle, U. Sterr, and C. Lisdat, "Realization of a timescale with an accurate optical lattice clock," Optica **3**, 563–569 (2016).

10. J. Lodewyck, S. Bilicki, E. Bookjans, J. L. Robyr, C. Shi, G. Vallet, R. Le Targat, D. Nicolodi, Y. Le Coq, J. Guéna, M. Abgrall, P. Rosenbusch, and S. Bize, "Optical to microwave clock frequency ratios with a nearly continuous strontium optical lattice clock," Metrologia **53**, 1123–1130 (2016).

11. H. Hachisu, F. Nakagawa, Y. Hanado, and T. Ido, "Months-long real-time generation of a time scale based on an optical clock," Sci. Rep. **8**, 4243 (2018).

12. J. Yao, T. E. Parker, N. Ashby, and J. Levine, "Incorporating an optical clock into a time scale," IEEE Trans. Ultrason. Ferroelectr. Freq. Control **65**, 127–134 (2018).

13. J. Yao, J. Sherman, T. Fortier, H. Leopardi, T. Parker, J. Levine, J. Savory, S. Romisch, W. McGrew, X. Zhang, D. Nicolodi, R. Fasano, S. Schaeffer, K. Beloy, and A. Ludlow, "Progress on optical-clock-based time scale at NIST: simulations and preliminary real-data analysis," Navigation **65**, 601–608 (2018).

14. P. Delva and J. Lodewyck, "Atomic clocks: new prospects in metrology and geodesy," Acta Futura **7**, 67–78 (2013).

15. P. Gill and F. Riehle, "On secondary representations of the second," in Proceedings of the 2006 Meeting of the European Frequency and Time Forum (2006), pp. 282–288.

16. F. Riehle, P. Gill, F. Arias, and L. Robertsson, "The CIPM list of recommended frequency standard values: guidelines and procedures," Metrologia **55**, 188–200 (2018).

17. H. Katori, M. Takamoto, V. G. Pal'chikov, and V. D. Ovsiannikov, "Ultrastable optical clock with neutral atoms in an engineered light shift trap," Phys. Rev. Lett. **91**, 173005 (2003).

18. N. D. Lemke, A. D. Ludlow, Z. W. Barber, T. M. Fortier, S. A. Diddams, Y. Jiang, S. R. Jefferts, T. P. Heavner, T. E. Parker, and C. W. Oates, "Spin-1/2 optical lattice clock," Phys. Rev. Lett. **103**, 063001 (2009).

19. T. M. Fortier, A. Bartels, and S. A. Diddams, "Octave-spanning Ti:sapphire laser with a repetition rate >1 GHz for optical frequency measurements and comparisons," Opt. Lett. **31**, 1011–1013 (2006).

20. J. E. Stalnaker, S. A. Diddams, T. M. Fortier, K. Kim, L. Hollberg, J. C. Bergquist, W. M. Itano, M. J. Delany, L. Lorini, W. H. Oskay, T. P. Heavner, S. R. Jefferts, F. Levi, T. E. Parker, and J. Shirley, "Optical-to-microwave frequency comparison with fractional uncertainty of 10^{-15}," Appl. Phys. B **89**, 167–176 (2007).

21. T. E. Parker, "Hydrogen maser ensemble performance and characterization of frequency standards," in Proceedings Joint Meeting of the IEEE International Frequency Control Symposium and the European Frequency and Time Forum, Besançon, France (1999), pp. 173–176.

22. Z. Jiang and G. Petit, "Combination of TWSTFT and GNSS for accurate UTC time transfer," Metrologia **46**, 305–314 (2009).

23. Y. Yao, Y. Jiang, H. Yu, Z. Bi, and L. Ma, "Optical frequency divider with division uncertainty at the 10^{-21} level," Natl. Sci. Rev. **3**, 463–469 (2016).

24. H. Leopardi, J. Davila-Rodriguez, F. Quinlan, J. Olson, J. A. Sherman, S. A. Diddams, and T. M. Fortier, "Single-branch Er:fiber frequency comb for precision optical metrology with 10^{-18} fractional instability," Optica **4**, 879–885 (2017).

25. J. A. Sherman and R. Jördens, "Oscillator metrology with software defined radio," Rev. Sci. Instrum. **87**, 054711 (2016).

26. https://www.bipm.org/en/bipm/tai/.

27. D.-H. Yu, M. Weiss, and T. E. Parker, "Uncertainty of a frequency comparison with distributed dead time and measurement interval offset," Metrologia **44**, 91–96 (2007).

28. J. Guéna, M. Abgrall, D. Rovera, P. Laurent, B. Chupin, M. Lours, G. Santarelli, P. Rosenbusch, M. E. Tobar, R. Li, K. Gibble, A. Clairon, and S. Bize, "Progress in atomic fountains at LNE-SYRTE," IEEE Trans. Ultrason. Ferroelectr. Freq. Control **59**, 391–409 (2012).

29. Y. S. Domnin, V. N. Baryshev, A. I. Boyko, G. A. Elkin, A. V. Novoselov, L. N. Kopylov, and D. S. Kupalov, "The MTsR-F2 fountain-type cesium frequency standard," Meas. Tech. **55**, 1155–1162 (2013).

30. F. Levi, D. Calonico, C. E. Calosso, A. Godone, S. Micalizio, and G. A. Costanzo, "Accuracy evaluation of ITCsF2: a nitrogen cooled caesium fountain," Metrologia **51**, 270–284 (2014).

31. J. Guéna, M. Abgrall, A. Clairon, and S. Bize, "Contributing to TAI with a secondary representation of the SI second," Metrologia **51**, 108–120 (2014).

32. F. Fang, M. Li, P. Lin, W. Chen, N. Liu, Y. Lin, P. Wang, K. Liu, R. Suo, and T. Li, "NIM5 Cs fountain clock and its evaluation," Metrologia **52**, 454–468 (2015).

33. S. Weyers, V. Gerginov, M. Kazda, J. Rahm, B. Lipphardt, G. Dobrev, and K. Gibble, "Advances in the accuracy, stability, and reliability of the PTB primary fountain clocks," Metrologia **55**, 789–805 (2018).

34. T. Kohno, M. Yasuda, K. Hosaka, H. Inaba, Y. Nakajima, and F. L. Hong, "One-dimensional optical lattice clock with a fermionic ^{171}Yb isotope," Appl. Phys. Express **2**, 072501 (2009).

35. M. Yasuda, H. Inaba, T. Kohno, T. Tanabe, Y. Nakajima, and K. Hosaka, "Improved absolute frequency measurement of the ^{171}Yb optical lattice clock towards the redefinition of the second," Appl. Phys. Express **5**, 102401 (2012).

36. C. Y. Park, D.-H. Yu, W.-K. Lee, S. E. Park, E. B. Kim, S. K. Lee, J. W. Cho, T. H. Yoon, J. Mun, S. J. Park, T. Y. Kwon, and S.-B. Lee, "Absolute frequency measurement of $^1S_0(F = 1/2)$-$^3P_0(F = 1/2)$ transition of ^{171}Yb atoms in a one-dimensional optical lattice at KRISS," Metrologia **50**, 119–128 (2013).

37. H. Kim, M.-S. Heo, W.-K. Lee, C. Y. Park, S.-W. Hwang, and D.-H. Yu, "Improved absolute frequency measurement of the ^{171}Yb optical lattice clock at KRISS relative to the SI second," Jpn. J. Appl. Phys. **56**, 050302 (2017).

38. M. Pizzocaro, P. Thoumany, B. Rauf, F. Bregolin, G. Milani, C. Clivati, G. A. Costanzo, F. Levi, and D. Calonico, "Absolute frequency measurement of the $^1S_0$-$^3P_0$ transition of ^{171}Yb," Metrologia **54**, 102–112 (2017).

39. H. S. Margolis and P. Gill, "Least-squares analysis of clock frequency comparison data to deduce optimized frequency and frequency ratio values," Metrologia **52**, 628–634 (2015).

40. A. D. Ludlow, M. M. Boyd, T. Zelevinsky, S. M. Foreman, S. Blatt, M. Notcutt, T. Ido, and J. Ye, "Systematic study of the ^{87}Sr clock transition in an optical lattice," Phys. Rev. Lett. **96**, 033003 (2006).

41. R. Le Targat, X. Baillard, M. Fouché, A. Brusch, O. Tcherbakoff, G. D. Rovera, and P. Lemonde, "Accurate optical lattice clock with ^{87}Sr atoms," Phys. Rev. Lett. **97**, 130801 (2006).

42. M. M. Boyd, A. D. Ludlow, S. Blatt, S. M. Foreman, T. Ido, T. Zelevinsky, and J. Ye, "^{87}Sr lattice clock with inaccuracy below 10^{-15}," Phys. Rev. Lett. **98**, 083002 (2007).

43. X. Baillard, M. Fouché, R. Le Targat, P. G. Westergaard, A. Lecallier, F. Chapelet, M. Abgrall, G. D. Rovera, P. Laurent, P. Rosenbusch, S. Bize, G. Santarelli, A. Clairon, P. Lemonde, G. Grosche, B. Lipphardt, and H. Schnatz, "An optical lattice clock with spin-polarized ^{87}Sr atoms," Eur. Phys. J. D **48**, 11–17 (2008).

44. G. K. Campbell, A. D. Ludlow, S. Blatt, J. W. Thomsen, M. J. Martin, M. H. G. De Miranda, T. Zelevinsky, M. M. Boyd, and J. Ye, "The absolute frequency of the ^{87}Sr optical clock transition," Metrologia **45**, 539–548 (2008).

45. F.-L. Hong, M. Musha, M. Takamoto, H. Inaba, S. Yanagimachi, A. Takamizawa, K. Watabe, T. Ikegami, M. Imae, Y. Fujii, M. Amemiya, K. Nakagawa, K. Ueda, and H. Katori, "Measuring the frequency of a Sr optical lattice clock using a 120 km coherent optical transfer," Opt. Lett. **34**, 692–694 (2009).

46. S. T. Falke, H. Schnatz, J. S. R. V. Winfred, T. H. Middelmann, S. T. Vogt, S. Weyers, B. Lipphardt, G. Grosche, F. Riehle, U. Sterr, and C. H. Lisdat, "The ^{87}Sr optical frequency standard at PTB," Metrologia **48**, 399–407 (2011).

47. A. Yamaguchi, N. Shiga, S. Nagano, Y. Li, H. Ishijima, H. Hachisu, M. Kumagai, and T. Ido, "Stability transfer between two clock lasers operating at different wavelengths for absolute frequency measurement of clock transition in ^{87}Sr," Appl. Phys. Express **5**, 022701 (2012).

48. R. Le Targat, L. Lorini, Y. Le Coq, M. Zawada, J. Guéna, M. Abgrall, M. Gurov, P. Rosenbusch, D. G. Rovera, B. Nagórny, R. Gartman, P. G. Westergaard, M. E. Tobar, M. Lours, G. Santarelli, A. Clairon, S. Bize, P. Laurent, P. Lemonde, and J. Lodewyck, "Experimental realization of an optical second with strontium lattice clocks," Nat. Commun. **4**, 2109 (2013).

49. D. Akamatsu, H. Inaba, K. Hosaka, M. Yasuda, A. Onae, T. Suzuyama, M. Amemiya, and F.-L. Hong, "Spectroscopy and frequency measurement of the ^{87}Sr clock transition by laser linewidth transfer using an optical frequency comb," Appl. Phys. Express **7**, 012401 (2014).

50. S. Falke, N. Lemke, C. Grebing, B. Lipphardt, S. Weyers, V. Gerginov, N. Huntemann, C. Hagemann, A. Al-Masoudi, S. Häfner, S. Vogt, U. Sterr, and C. Lisdat, "A strontium lattice clock with 3 × 10^{-17} inaccuracy and its frequency," New J. Phys. **16**, 073023 (2014).

51. T. Tanabe, D. Akamatsu, T. Kobayashi, A. Takamizawa, S. Yanagimachi, T. Ikegami, T. Suzuyama, H. Inaba, S. Okubo, M. Yasuda, F. L. Hong, A. Onae, and K. Hosaka, "Improved frequency measurement of the $^{1}S_{0}$-$^{3}P_{0}$ clock transition in ^{87}Sr using a Cs fountain clock as a transfer oscillator," J. Phys. Soc. Jpn. **84**, 115002 (2015).

52. Y.-G. Lin, Q. Wang, Y. Li, F. Meng, B.-K. Lin, E.-J. Zang, Z. Sun, F. Fang, T.-C. Li, and Z.-J. Fang, "First evaluation and frequency measurement of the strontium optical lattice clock at NIM," Chin. Phys. Lett. **32**, 090601 (2015).

53. H. Hachisu, G. Petit, F. Nakagawa, Y. Hanado, and T. Ido, "SI-traceable measurement of an optical frequency at the low 10^{-16} level without a local primary standard," Opt. Express **25**, 8511–8523 (2017).

54. H. Hachisu, G. Petit, and T. Ido, "Absolute frequency measurement with uncertainty below 1×10^{-15} using International Atomic Time," Appl. Phys. B **123**, 34 (2017).

55. D. Akamatsu, M. Yasuda, H. Inaba, K. Hosaka, T. Tanabe, A. Onae, and F.-L. Hong, "Frequency ratio measurement of ^{171}Yb and ^{87}Sr optical lattice clocks," Opt. Express **22**, 7898–7905 (2014).

56. M. Takamoto, I. Ushijima, M. Das, N. Nemitz, T. Ohkubo, K. Yamanaka, N. Ohmae, T. Takano, T. Akatsuka, A. Yamaguchi, and H. Katori, "Frequency ratios of Sr, Yb, and Hg based optical lattice clocks and their applications," C. R. Physique **16**, 489–498 (2015).

57. N. Nemitz, T. Ohkubo, M. Takamoto, I. Ushijima, M. Das, N. Ohmae, and H. Katori, "Frequency ratio of Yb and Sr clocks with 5×10^{-17} uncertainty at 150 seconds averaging time," Nat. Photonics **10**, 258–261 (2016).

58. J. Grotti, S. Koller, S. Vogt, S. Häfner, U. Sterr, C. Lisdat, H. Denker, C. Voigt, L. Timmen, A. Rolland, F. N. Baynes, H. S. Margolis, M. Zampaolo, P. Thoumany, M. Pizzocaro, B. Rauf, F. Bregolin, A. Tampellini, P. Barbieri, M. Zucco, G. A. Costanzo, C. Clivati, F. Levi, and D. Calonico, "Geodesy and metrology with a transportable optical clock," Nat. Phys. **14**, 437–441 (2018).

59. D. Akamatsu, T. Kobayashi, Y. Hisai, T. Tanabe, K. Hosaka, M. Yasuda, and F.-L. Hong, "Dual-mode operation of an optical lattice clock using strontium and ytterbium atoms," IEEE Trans. Ultrason. Ferroelectr. Freq. Control **65**, 1069–1075 (2018).

60. M. Fujieda, S. Yang, T. Gotoh, S. Hwang, H. Hachisu, H. Kim, Y. Lee, R. Tabuchi, T. Ido, W. Lee, M. Heo, C. Y. Park, D. Yu, and G. Petit, "Advanced satellite-based frequency transfer at the 10^{-16} level," IEEE Trans. Ultrason. Ferroelectr. Freq. Control **65**, 973–978 (2018).

61. M. S. Safronova, D. Budker, D. DeMille, D. F. J. Kimball, A. Derevianko, and C. W. Clark, "Search for new physics with atoms and molecules," Rev. Mod. Phys. **90**, 025008 (2017).

62. V. V. Flambaum and A. F. Tedesco, "Dependence of nuclear magnetic moments on quark masses and limits on temporal variation of fundamental constants from atomic clock experiments," Phys. Rev. C **73**, 055501 (2006).

63. V. V. Flambaum and V. A. Dzuba, "Search for variation of the fundamental constants in atomic, molecular, and nuclear spectra," Can. J. Phys. **87**, 25–33 (2009).

64. T. H. Dinh, A. Dunning, V. A. Dzuba, and V. V. Flambaum, "Sensitivity of hyperfine structure to nuclear radius and quark mass variation," Phys. Rev. A **79**, 054102 (2009).

65. V. A. Dzuba and V. V. Flambaum, "Limits on gravitational Einstein equivalence principle violation from monitoring atomic clock frequencies during a year," Phys. Rev. D **95**, 015019 (2017).

66. N. Ashby, T. E. Parker, and B. R. Patla, "A null test of general relativity based on a long-term comparison of atomic transition frequencies," Nat. Phys. **14**, 822–826 (2018).

67. T. Rosenband, D. B. Hume, P. O. Schmidt, C. W. Chou, A. Brusch, L. Lorini, W. H. Oskay, R. E. Drullinger, T. M. Fortier, J. E. Stalnaker, S. A. Diddams, W. C. Swann, N. R. Newbury, W. M. Itano, D. J. Wineland, and J. C. Bergquist, "Frequency ratio of Al^{+} and Hg^{+} single-ion optical clocks; metrology at the 17th decimal place," Science **319**, 1808–1812 (2008).

68. S. Peil, S. Crane, J. L. Hanssen, T. B. Swanson, and C. R. Ekstrom, "Tests of local position invariance using continuously running atomic clocks," Phys. Rev. A **87**, 010102 (2013).

optica

Towards the optical second: verifying optical clocks at the SI limit: supplementary material

W. F. McGrew,[1,2] X. Zhang,[1] H. Leopardi,[1,2] R. J. Fasano,[1,2] D. Nicolodi,[1,2] K. Beloy,[1] J. Yao,[1,2]

J. A. Sherman,[1] S. A. Schäffer,[1,*] J. Savory,[1] R. C. Brown,[1,†] S. Römisch,[1] C. W. Oates,[1]

T. E. Parker,[1,‡] T. M. Fortier,[1,§] A. D. Ludlow[1,2,¶]

[1]*National Institute of Standards and Technology, 325 Broadway, Boulder, Colorado 80305, USA*
[2]*Department of Physics, University of Colorado, Boulder, Colorado 80309, USA*
*Permanent address: Niels Bohr Institute, University of Copenhagen, Blegdamsvej 17, 2100 Copenhagen, Denmark
†Present address: Georgia Tech Research Institute, Atlanta, Georgia 30332, USA
‡tom.parker@nist.gov
§tara.fortier@nist.gov
¶andrew.ludlow@nist.gov

This document provides supplementary information to "Towards the optical second: verifying optical clocks at the SI limit," https://doi.org/10.1364/OPTICA.6.000448.

A. Frequency connection to AT1E and dead time uncertainty

After determination of the normalized fractional frequency difference y(Yb−ST15), the difference between ST15 and the AT1E and AT1 maser time scales is measured, where AT1E is a post-processed time scale that uses the same algorithm and clock measurement data as the real-time time scale AT1 (identified by the BIPM as TA(NIST)) [1]. Since AT1E is post-processed, it has generally better stability than AT1 because clocks suffering from environmental perturbations and other technical anomalies can be de-weighted before the problem actually occurs. In both AT1 and AT1E the maser frequency drift rates are modeled in the time scale algorithm by using PSFS data from Circular T. AT1E has a frequency drift rate more than a factor of 100 smaller than that of ST15. The BIPM provides time difference data for AT1 relative to International Atomic Time (TAI) [2]. The BIPM also provides a monthly (typically 30 days, but sometimes 25 or 35 days) average frequency of TAI as measured by primary and secondary frequency standards (PSFS) located in national metrology laboratories around the world. We note that PSFS, which is derived from a group of frequency standards, is preferable to TAI, a time scale, as it does not include frequency steps to correct for past time deviations. The frequency difference information is available in Circular T [2], which is published once a month. Thus, there is a chain of frequency ratio data from the Yb standard to ST15, to AT1E, to AT1, to TAI, and finally to PSFS. However, the Yb standard is operated only intermittently, and thus there is considerable dead time in the first step of this transfer.

The runs in a month are not distributed evenly. Therefore, the mean time of the runs will not align with the midpoint of the month. Thus, any frequency drift in AT1E will cause a small frequency offset between the mean frequency and what it would be at the midpoint. The frequency drift over the eight month period of interest is less than 7×10^{-18}/day. The offsets between mean time and midpoint for each month are approximately randomly distributed about zero, with the largest being -9.1 days and the average being -0.4 days. Thus, the average frequency offset due to AT1E drift is well below 1×10^{-17}. Another issue that arose was the presence of an excess number of outliers in the ten (one) second-gated counter (SDR) data. Ninety 5σ outliers are found for the entire dataset, where < 1 are expected from Gaussian statistics. The outliers could potentially bias the mean through an asymmetric distribution. In order to constrain this asymmetry, the Pearson skew is calculated for each individual dataset [3]. No correlation is found between the skew of a given set and the density of outliers found within that set, leading to

a constraint on the role of outliers in data skew at the level of $< 3 \times 10^{-17}$.

Because ST15 operates as a transfer oscillator, its noise does not directly impact the measurement of Yb against PSFS. However, it is necessary to determine the inherent statistical uncertainty arising from the ytterbium clock, frequency comb, and measurement system linked to ST15. This error, denoted here as σ_{Yb}, is generally expected to be very low (e.g. at 1,000 s of averaging, $< 1 \times 10^{-19}$ for the comb [4] and $< 1 \times 10^{-17}$ for the atomic system [5]), but a conservative upper bound is assessed by comparing ST15 noise as measured by the NIST time scale and the Yb/comb system. Measurements of y(Yb−ST15) show that the observed Allan deviation, $\sigma_{\mathrm{Yb-ST15}} = \sqrt{\sigma_{\mathrm{Yb}}^2 + \sigma_{\mathrm{ST15}}^2}$, is essentially the same as what is observed for ST15 when measured against AT1E, $\sigma_{\mathrm{ST15-AT1E}}$. Since ST15 contributes to AT1E with weight $w_{\mathrm{ST15}} \approx 10\text{–}15\%$, it is necessary to account for covariance: $\sigma_{\mathrm{ST15}} = \frac{\sigma_{\mathrm{ST15-AT1E}}}{(1-w_{\mathrm{ST15}})^{1/2}}$ [6]. More specifically, given the statistical confidence levels for such measurements, the two Allan deviations differ at no more than the 10% level, $\sigma_{\mathrm{Yb-ST15}} \lesssim 1.1\sigma_{\mathrm{ST15}}$. This implies that σ_{Yb} cannot be larger than about one half of the noise of the maser, $\sigma_{\mathrm{Yb}} = \sqrt{\sigma_{\mathrm{Yb-ST15}}^2 - \sigma_{\mathrm{ST15}}^2} \lesssim 0.5\,\sigma_{\mathrm{ST15}}$. The minimum measurement interval of AT1 data is 720 s, and the maser noise level at this interval is 2.7×10^{-15}. This gives an upper limit to the noise at 720 s of $\sigma_{\mathrm{Yb}} \approx 1.4 \times 10^{-15}$, or 1.3×10^{-16} at 1 day. A three-corner hat analysis can also be used to determine σ_{ST15}, but it leads to worse confidence limits.

The NIST time scale measurement system provides a time difference measurement between the maser ST15 and AT1E on a twelve-minute (720 s) grid. The noise level of a time difference measurement of any length relevant to this study is 1 ps, which contributes a fractional frequency uncertainty of $\sigma_{\mathrm{ts}} = 1.4 \times 10^{-15}/n$ for a measurement spanning n consecutive twelve-minute bins. The time scale measurement noise, as listed in Table 1 amounts to $< 1 \times 10^{-17}$ for the full measurement campaign. Another fact to consider is that the y(Yb−ST15) measurements do not start and stop on the twelve-minute grid. All data points that fall within a given twelve-minute span are averaged together to project the measurements onto the grid. If the uptime during a given gridpoint is less than 100%, additional dead time uncertainty, σ_{dt}, is added to this datapoint, increasing the statistical uncertainty associated with this point. Dead time uncertainty is added by using Eq. (2) of Ref. [7], which makes use of Eq. (8) of Ref. [8], and this equation requires knowledge of the noise model of ST15. For an averaging time of 720 s, ST15 can be treated as having a mixed white FM and white PM noise model, and the one-second instabilities of these terms are measured to be $(62 \pm 4) \times 10^{-15}$ and $(202 \pm 6) \times 10^{-15}$, respectively. Dead time varies for each twelve-minute gridpoint, depending on uptime. For instance, a unity uptime corresponds to $\sigma_{\mathrm{dt}} = 0$, and an uptime of 10% corresponds to $\sigma_{\mathrm{dt}} = 8 \times 10^{-15}$. The total uncertainty of the Yb-maser comparison, as listed in Table 1, consists of σ_{Yb} as well as σ_{dt} and amounts to 4×10^{-17} for the full measurement.

Thus, we have transformed the intermittent y(Yb−ST15) measurements to the twelve-minute-gridded $\mathrm{y}_{\text{12-min}}$(Yb−ST15), and for each measurement we have a corresponding $\mathrm{y}_{\text{12-min}}$(ST15−AT1E) measurement with no dead time. From these, we calculate $\mathrm{y}_{\text{12-min}}$(Yb−AT1E). The next step is to calculate the weighted mean of all runs that occur in a month to obtain the average frequency difference between the Yb standard and AT1E for a month corresponding to the Modified Julian Dates (MJDs) of the Circular T data. We will identify this average value as $\mathrm{y_m}$(Yb−AT1E). The weighting factor of each contributing 12-minute gridpoint is given by the inverse-square of the uncertainties (σ_{Yb}, σ_{ts}, and σ_{dt}) of that point.

There is considerable dead time uncertainty associated with $\mathrm{y_m}$(Yb−AT1E), because the 720-s grid of $\mathrm{y}_{\text{12-min}}$(Yb−AT1E) is sparsely populated. The dead time uncertainty is calculated using the method of Ref. [7] for distributed dead time, but the noise characteristics of AT1E must be known in order to calculate this. Fig. 1 shows the results of a three-corner hat analysis between AT1E and two independent masers not in AT1E. Confidence limits are not available with the software used to calculate the three-corner hat. The components of the noise model
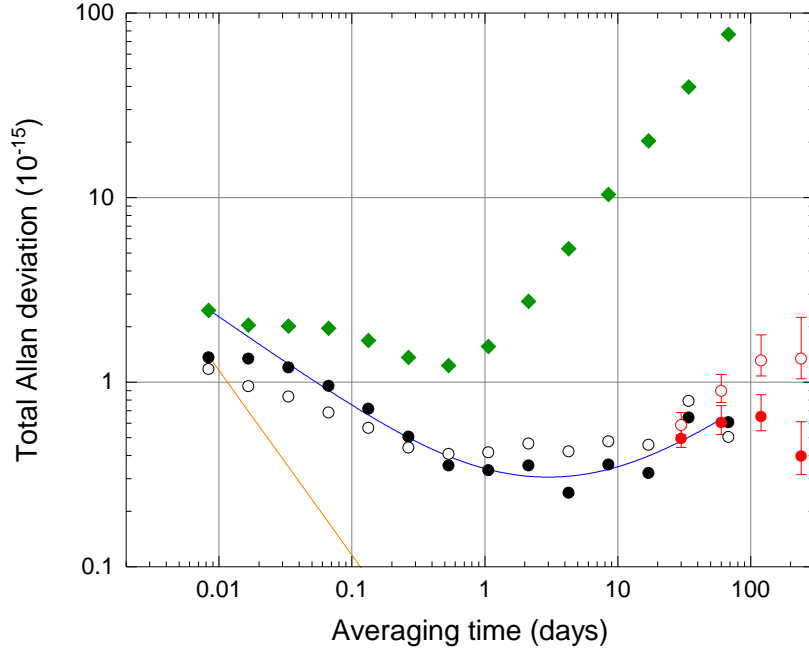
Fig. 1. Noise characteristics of relevant frequency references. Filled (empty) circles represent the Allan deviation of AT1E (AT1). Black datapoints are determined by a three-corner hat analysis with hydrogen masers ST11 and ST4, and red datapoints are determined by comparison with Circular T data of PSFS frequencies. Green diamonds are the Allan deviation of ST15, determined by a three-corner hat analysis with ST5 and ST22. AT1E averages down at >100 days because y(AT1E−PSFS) is used to loosely steer AT1E. The blue line is a fit to a mixed-noise model of AT1E; see main text. The orange line is the time scale measurement uncertainty, σ_{ts}.

are taken to be white FM, flicker FM, and random walk FM added in quadrature. A fit of the total Allan deviation out to 60 days was performed, and the magnitudes of the total Allan deviation at one day for each component are $(2.25 \pm 0.11) \times 10^{-16}$, $(2.45 \pm 0.46) \times 10^{-16}$, and $(0.750 \pm 0.085) \times 10^{-16}$, respectively. The three-corner hat analysis was performed for a 260 day interval covering approximately the eight month interval of the Yb measurements. This dead time uncertainty represents the largest single source of statistical error for a single month, ranging from 2.0×10^{-16} to 4.6×10^{-16} for the individual months that make up the measurement campaign. Stability plots for AT1 and ST15 are also shown in Fig. 4. The dead time uncertainty is smaller using AT1E than for AT1.

An alternative, but similar, method to that described above was also used. Here the y(Yb−AT1E) data was placed in one-day bins, rather than 720 s bins, then combined into monthly averages with dead time uncertainties assigned based on the daily bins. The results for this method are $y_T(\text{Yb}-\text{PSFS}) = (1.7 \pm 2.1) \times 10^{-16}$, with $\chi^2_{\text{red}} = 1.28$, which agrees well with the result reported in the main text, $y_T(\text{Yb}-\text{PSFS}) = (2.1 \pm 2.1) \times 10^{-16}$.

B. Frequency connection to PSFS

The frequency differences must now be transferred from AT1E to AT1, as the BIPM only receives timing data from the latter time scale. NIST time scale data are used to obtain y(AT1−AT1E) with uncertainties at the 1×10^{-17} level. The fact that there is any uncertainty in y(AT1−AT1E) stems from the fact that AT1E and AT1 handle clock anomalies differently [1]. The next step is to calculate y_m(AT1−PSFS) using data from the BIPM. The AT1 time scale is transferred to the BIPM using the hybrid Two-Way Satellite Time and Frequency Transfer/GPS Precise Point Positioning (TWGPPP) frequency transfer protocol [9]. The frequency transfer uncertainty in this value can be calculated from Eq. (25) in Ref. [10] and amounts to 3.1×10^{-16}, 2.6×10^{-16}, and 2.3×10^{-16} for months with lengths of 25, 30, and 35 days, respectively, where we have used the type A uncertainty of 0.4 ns for TAI-AT1 in Circular T [2]. The type B uncertainty of TAI-AT1 in Circular T represents an unknown constant time offset between the two time scales and is irrelevant for frequency comparisons such as those reported here. The transfer uncertainty represents the second largest source of statistical uncertainty, after dead time uncertainty. It is also necessary to transform the clock frequency into the reference surface of the geoid by correcting for the relativistic redshift. This is done with an uncertainty of 6×10^{-18} using the geopotential determination from a recent geodetic survey [11]. Each month the BIPM publishes values for y_m(AT1−TAI) as well as y_m(TAI−PSFS) [2]. Thus, we have finally,

$$y_m(Yb - PSFS) = y_m(Yb - AT1E) + y_m(AT1E - AT1) + y_m(AT1 - TAI) + y_m(TAI - PSFS),$$
(1)

where all y_m are for the same time interval (25, 30, or 35 days). The uncertainty budget is listed in Table 1, displaying the uncertainties associated with the month of March, as well as for the full campaign.

The type A (statistical) and type B (systematic) uncertainties for each primary and secondary frequency standard reporting are given in Circular T for a specific time interval. In addition to the individual standards, a total uncertainty for the weighted mean of y(TAI−PSFS) is also given. This total uncertainty is calculated from the type A and B uncertainties of the individual standards, as well as the uncertainty in transferring frequency information from each standard to TAI. We make the conservative assumption that the type B uncertainty of the PSFS ensemble does not average over time. For individual months during our measurement campaign, the type B uncertainty of PSFS, $u_B(t)$, ranged between 1.0×10^{-16} and 1.7×10^{-16}. The average value, $\overline{u_B(t)}$, is 1.3×10^{-16}. During the course of the eight month measurement, ten separate standards contributed to PSFS: two Cs thermal beam clocks (PTB-CS1 and PTB-CS2), seven Cs fountains (PTB-CsF1, PTB-CsF2, SYRTE FO1, SYRTE FO2, SU-CsF2, IT-CsF2, and NIM5) [12–16], and a single Rb fountain (SYRTE FORb) [17], with between five and eight of these being present in any given month. The SYRTE and PTB Cs fountains were present most often and have the most weight.

An alternative approach to that described above was also used to compare Yb against PSFS via the chain of Yb→AT1→TAI→PSFS. Instead of processing the data monthly, this approach treats each optical clock run individually and then processes the full-campaign data all together. First, we determine the frequency difference y_r(Yb−AT1) for a given run. Then, this value is added to y_{avg}(AT1−TAI), the average frequency difference between the NIST time scale and TAI, which is published on a 5-day grid. This step adds long-term noise from the frequency transfer techniques from NIST to the BIPM. Each of the runs, y_r(Yb−TAI), are averaged together to yield y_T(Yb−TAI). However, since dead-time uncertainty has not been yet accounted for, the points are overscattered, and the uncertainty of the mean is expanded by $\sqrt{\chi^2_{red}} = 1.6$. The resultant mean is added to y_T(TAI−PSFS), published by the BIPM. This approach yields the frequency difference y_T(Yb−PSFS) $= (2.0 \pm 2.0) \times 10^{-16}$, in good agreement with the results in the main
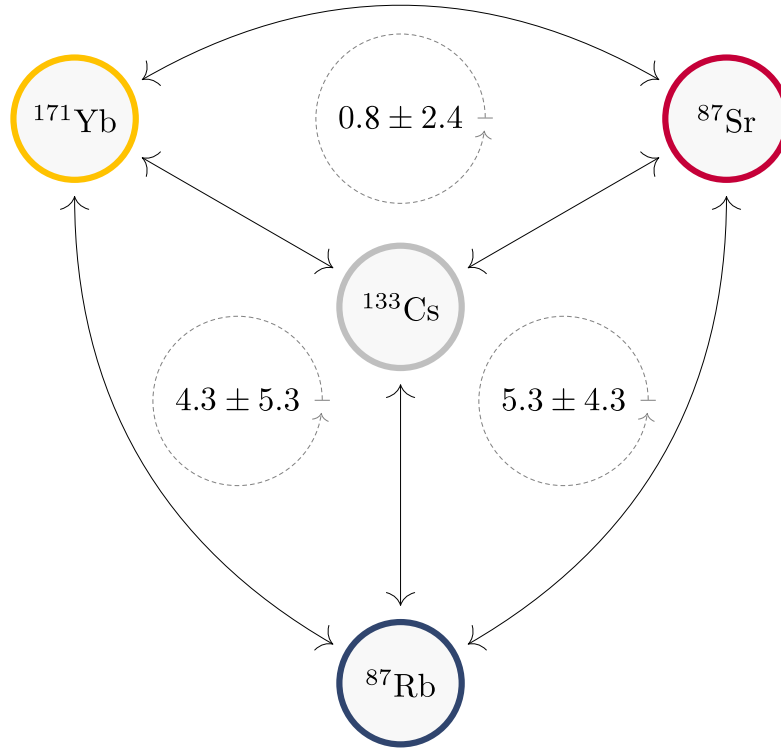
Fig. 2.   Diagram representing three loop closures involving optical frequency standards and microwave frequency standards. The numbers represent the loop misclosure (as parts in 10^{16}), as defined in the main text. Comparisons are represented by connections between the standards. The contributing Yb absolute frequency measurements were from NIST, INRIM, KRISS, NMIJ; Sr absolute measurements from PTB, SYRTE, NICT, JILA, NMIJ, NIM, UT; Rb absolute measurements from NPL, SYRTE; Yb/Sr optical ratios from RIKEN, PTB/INRIM, NMIJ, KRISS/NICT; Yb/Rb ratio from NIST; Sr/Rb ratio from SYRTE.

text, y_T(Yb−PSFS) = $(2.1 \pm 2.1) \times 10^{-16}$. This good agreement using a very different analysis method demonstrates that the results in the main text are robust against alternative methods of analysis.

C.   Yb/Rb ratio and further loop closures

A single secondary representation of the second, the ^{87}Rb hyperfine transition, contributed to PSFS over this eight-month period [17], though the relatively high uncertainty (6×10^{-16}) given by the CIPM to this transition meant that its impact was negligible relative to the Cs fountains [18]. However, since the frequency difference from TAI is given for each individual standard, it is possible to determine y_m(Yb−SYRTE FORb), allowing a determination of the Yb-Rb frequency ratio. The SYRTE FORb frequency standard contributed for three of the eight months, for a combined total Yb-Rb runtime of 3.3 days. The type A uncertainty for the three months is 3.3×10^{-16}, and the type B uncertainty of the standard was 2.7×10^{-16}, leading to a total uncertainty of 4.3×10^{-16}. The ratio is found to be ν_{Yb}/ν_{Rb} =75 833.197 545 114 192(33). This agrees well with $\nu_{Yb}^{CIPM17}/\nu_{Rb}^{CIPM17}$ =75 833.197 545 114 196(59). For the Yb/Rb

measurements, $\chi^2_{\text{red}} = 0.72$.

Table 1. Loop closures performed on the Cs-X-Y-Cs loop, where X and Y are frequency standards.

X	Y	X/Cs ref.	Y/Cs ref.	X/Y ref.	Misclosure (10^{-16})
^{171}Yb	^{87}Sr	this work, [19–24]	[25–41],	[42–47]	0.8 ± 2.4
^{171}Yb	^{87}Rb	"	[2, 48, 49]	this work	4.3 ± 5.3
^{87}Sr	^{87}Rb	[25–41],	"	[38]	5.3 ± 4.3
^{87}Sr	^{199}Hg	"	[50, 51]	[51, 52]	-1.6 ± 4.5
^{87}Sr	^{88}Sr	"	[53, 54]	[55–57]	-21 ± 40
^{87}Sr	^{40}Ca$^+$	"	[58–61]	[59]	48 ± 50
^{199}Hg	^{87}Rb	[50, 51]	[2, 48, 49]	[51]	4.8 ± 6.1
^{171}Yb$^+$E2	^{171}Yb$^+$E3	[62–65]	[65–70]	[65]	-14.0 ± 5.6
^{27}Al$^+$	^{199}Hg$^+$	[71]	[72]	[73]	-57 ± 54
^{40}Ca	^{199}Hg$^+$	[74, 75]	"	[76]	-100 ± 760

The measurement of the Yb/Rb ratio allows the determination of two additional frequency loop misclosures; see Fig. 2. The Rb absolute frequency is determined as $\nu_{\text{Rb}} = 6\,834\,682\,610.904\,311\,5(16)$ Hz, by a weighted average of three previous measurements [2, 48, 49]. The displayed Yb/Rb ratio is from this work, and the Sr/Rb ratio is from [38]. In each of the three loops examined (Yb/Sr, Yb/Rb, Sr/Rb), misclosures are consistent with zero at an uncertainty smaller than 6×10^{-16}. In Table 1, we compile a list of all loops that have been closed with Cs as one of the three points. As expected from statistics, three of the ten loops are at least 1σ from zero. Only a single loop has a misclosure $> 2\sigma$ from zero.

D. Constraints on variations of constants from Yb and Sr absolute frequency measurements

To tighten the contraints on the possible variations of fundamental constants, we employ a multi-species analysis that can be used to link absolute frequency measurements of different types of atomic clocks with optical ratios that have been measured with sufficient precision. We link our results with prior absolute measurements of the ^{171}Yb and ^{87}Sr transition frequencies. First, we multiply the Sr transition frequency by the well-known ratio, $\mathcal{R}_{\text{opt}}^{\text{avg}} = 1.207\,507\,039\,343\,337\,768(60)$, derived from Refs [42–47] as described in the main text. The ratio is known with a fractional uncertainty of $\sigma_{\text{stat}} = 5.6 \times 10^{-17}$. However, care must be taken during this step due to the non-zero sensitivity of the Yb/Sr ratio to variation of the fine structure constant (N.B.: $\Delta K_{\text{Yb,Sr}}^{X_q} = \Delta K_{\text{Yb,Sr}}^{\mu} = 0$). Prior analyses have constrained $\frac{\dot{\alpha}}{\alpha}$ to be consistent with zero at the level of 2×10^{-17}/yr [65, 69], and $k_\alpha(\frac{\Delta\Phi}{c^2})$ to be consistent with zero at the level of 1.7×10^{-17} [77]. Multiplying these numbers by $\Delta K_{\text{Yb,Sr}}^{\alpha} = 0.25$, we obtain a constraint on the time-variation of the Yb-Sr ratio of $< 5 \times 10^{-18}$/yr and a constraint on gravitational potential-variation of $\sigma_{\text{grav}} = 4 \times 10^{-18}$. To account for a possible drift in α in a conservative fashion, we multiply the former number by twelve years, the entire duration of the record of absolute frequency measurements, leading to $\sigma_{\text{time}} = 6 \times 10^{-17}$. Finally, we expand the error bars of each of the rescaled Sr absolute frequency measurements by $\sqrt{\sigma_{\text{stat}}^2 + \sigma_{\text{grav}}^2 + \sigma_{\text{time}}^2} = 8.2 \times 10^{-17}$. For all Sr
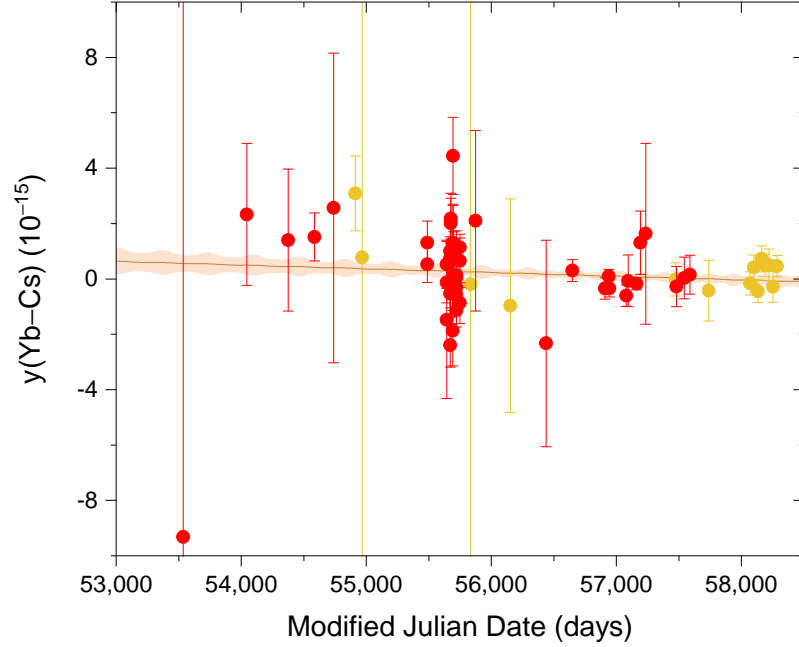
Fig. 3. A summary of this work, as well as six other Yb absolute frequency measurements (yellow) [19–24], and seventeen Sr measurements (red) [25–41]. Sr measurements are multiplied by the Yb/Sr ratio and the error bars are expanded as descibed in the main text. The fit function (orange) constrains possible variation of the Yb/Cs ratio, and the shaded region represents the 1σ uncertainty of the fit.

measurements, this increased uncertainty had only a slight impact upon the initial error bar, the lowest of which was 2.6×10^{-16}, or 2.7×10^{-16} after rescaling [39].

The seven Yb measurements [19–24] and 17 rescaled Sr measurements [25–41] are displayed in Fig. 3. For Refs. [33, 38, 41], measurements took place over many months, and so individual runs were extracted from the published work, rather than simply using the average. In order to constrain variation of constants arising from both time and gravitational potential, we fit the function $y(\text{Yb}-\text{Cs}) = A\cos(2\pi\frac{t-t_0}{1\,\text{yr}}) + \dot{y}t + y_0$, where t is the date. A, $\dot{y}$, and y_0 are free parameters. We determine $A = (0.1 \pm 1.5) \times 10^{-16}$ and $\dot{y} = (-4.9 \pm 3.6) \times 10^{-17}/\text{yr}$. The Yb/Cs measurements and rescaled Sr/Cs measurements are sensitive to variations of α, X_q, and μ.

Using the values in Table 2 and the amplitude of the sinusoidal fit, we find $k_\mu = (-0.19 \pm 0.94) \times 10^{-6}$, indicating a constraint a factor of 1.5 below the constraint derived from our measurements alone. We also use the linear fit to constrain the drift of μ by using the equation, $\dot{y} = \sum_\epsilon \Delta K^\epsilon_{\text{Yb,Cs}} \frac{\dot{\epsilon}}{\epsilon}$. We note that, using the values of $\dot{\alpha}$ and $\dot{X}_q$ from Ref. [65] and Ref. [12], $\Delta K^\alpha_{\text{Yb,Cs}}(\frac{\dot{\alpha}}{\alpha}) = (1.8 \pm 5.3) \times 10^{-17}/\text{yr}$ and $\Delta K^{X_q}_{\text{Yb,Cs}}(\frac{\dot{X}_q}{X_q}) = (-1.4 \pm 0.9) \times 10^{-17}/\text{yr}$. Solving for μ, we find that $\frac{\dot{\mu}}{\mu} = (5.3 \pm 6.5) \times 10^{-17}/\text{yr}$. This represents an improvement of almost a factor of two below the previous constraint, $\frac{\dot{\mu}}{\mu} = (-2 \pm 11) \times 10^{-17}/\text{yr}$ [65].

References

1. T. E. Parker, "Hydrogen Maser Ensemble Performance and Characterization of Frequency Standards," in *Proceedings 1999 Joint Meeting of the IEEE International Frequency Control Symposium and the European Frequency and Time Forum (Besancon),* (1999), pp. 173–176.

2. www.bipm.org/en/bipm/tai/.

3. B. Harding, C. Tremblay, and D. Cousineau, "The standard error of the Pearson skew," *The Quant. Methods for Psychol.* **11**, 32–36 (2015).

4. H. Leopardi, J. Davila-Rodriguez, F. Quinlan, J. Olson, J. A. Sherman, S. A. Diddams, and T. M. Fortier, "Single-branch Er:fiber frequency comb for precision optical metrology with 10^{-18} fractional instability," *Optica* **4**, 879–885 (2017).

5. M. Schioppo, R. C. Brown, W. F. McGrew, N. Hinkley, R. J. Fasano, K. Beloy, T. H. Yoon, G. Milani, D. Nicolodi, J. A. Sherman, N. B. Phillips, C. W. Oates, and A. D. Ludlow, "Ultra-stable optical clock with two cold-atom ensembles," *Nat. Photonics* **11**, 48–52 (2016).

6. P. Tavella, J. Azoubib, and C. Thomas, "Study of the clock-ensemble correlation in ALGOS using real data," in *Proceedings of the 5th European Frequency and Time Forum Besancon,* (1991), pp. 435–441.

7. D.-H. Yu, M. Weiss, and T. E. Parker, "Uncertainty of a frequency comparison with distributed dead time and measurement interval offset," *Metrologia* **44**, 91–96 (2007).

8. R. J. Douglas and J. Boulanger, "Standard uncertainty for average frequency traceability," in *Proceedings of the 11th European Frequency and Time Forum (Neuchatel),* (1997), pp. 345–349.

9. Z. Jiang and G. Petit, "Combination of TWSTFT and GNSS for accurate UTC time transfer," *Metrologia* **46**, 305–314 (2009).

10. G. Panfilo and T. E. Parker, "A theoretical and experimental analysis of frequency transfer uncertainty, including frequency transfer into TAI," *Metrologia* **47**, 552–560 (2010).

11. N. K. Pavlis and M. A. Weiss, "A re-evaluation of the relativistic redshift on frequency standards at NIST, Boulder, Colorado, USA," *Metrologia* **54**, 535–548 (2017).

12. J. Guéna, M. Abgrall, D. Rovera, P. Laurent, B. Chupin, M. Lours, G. Santarelli, P. Rosenbusch, M. E. Tobar, R. Li, K. Gibble, A. Clairon, and S. Bize, "Progress in atomic fountains at LNE-SYRTE," *IEEE Transactions on Ultrason. Ferroelectr. Freq. Control.* **59**, 391–410 (2012).

13. Y. S. Domnin, V. N. Baryshev, A. I. Boyko, G. A. Elkin, A. V. Novoselov, L. N. Kopylov, and D. S. Kupalov, "The MTsR-F2 Fountain-Type Cesium Frequency Standard," *Meas. Tech.* **55**, 1155–1162 (2013).

14. F. Levi, D. Calonico, C. E. Calosso, A. Godone, S. Micalizio, and G. A. Costanzo, "Accuracy evaluation of ITCsF2: A nitrogen cooled caesium fountain," *Metrologia* **51**, 270–284 (2014).

15. F. Fang, M. Li, P. Lin, W. Chen, N. Liu, Y. Lin, P. Wang, K. Liu, R. Suo, and T. Li, "NIM5 Cs fountain clock and its evaluation," *Metrologia* **52**, 454–468 (2015).

16. S. Weyers, V. Gerginov, M. Kazda, J. Rahm, B. Lipphardt, G. Dobrev, and K. Gibble, "Advances in the accuracy, stability, and reliability of the PTB primary fountain clocks," *Metrologia* **55**, 789–805 (2018).

17. J. Guéna, M. Abgrall, A. Clairon, and S. Bize, "Contributing to TAI with a secondary representation of the SI second," *Metrologia* **51**, 108–120 (2014).

18. F. Riehle, P. Gill, F. Arias, and L. Robertsson, "The CIPM list of recommended frequency standard values: guidelines and procedures," *Metrologia* **55**, 188–200 (2018).

19. N. D. Lemke, A. D. Ludlow, Z. W. Barber, T. M. Fortier, S. A. Diddams, Y. Jiang, S. R. Jefferts, T. P. Heavner, T. E. Parker, and C. W. Oates, "Spin-1/2 optical lattice clock," *Phys. Rev. Lett.* **103**, 063001 (2009).

20. T. Kohno, M. Yasuda, K. Hosaka, H. Inaba, Y. Nakajima, and F. L. Hong, "One-dimensional optical lattice clock with a fermionic ^{171}Yb isotope," *Appl. Phys. Express* **2**, 072501 (2009).

21. M. Yasuda, H. Inaba, T. Kohno, T. Tanabe, Y. Nakajima, and K. Hosaka, "Improved Absolute Frequency Measurement of the ^{171}Yb Optical Lattice Clock towards the Redefinition of the Second," *Appl. Phys. Express* **5**, 102401 (2012).

22. C. Y. Park, D.-H. Yu, W.-K. Lee, S. E. Park, E. B. Kim, S. K. Lee, J. W. Cho, T. H. Yoon, J. Mun, S. J. Park, T. Y. Kwon, and S.-B. Lee, "Absolute frequency measurement of $^1S_0(F = 1/2)$–$^3P_0(F = 1/2)$ transition of ^{171}Yb atoms in a one-dimensional optical lattice at KRISS," *Metrologia* **50**, 119–128 (2013).

23. H. Kim, M.-S. Heo, W.-K. Lee, C. Y. Park, S.-W. Hwang, and D.-H. Yu, "Improved absolute frequency measurement of the ^{171}Yb optical lattice clock at KRISS relative to the SI second," *Jpn. J. Appl. Phys.* **56**, 050302 (2017).

24. M. Pizzocaro, P. Thoumany, B. Rauf, F. Bregolin, G. Milani, C. Clivati, G. A. Costanzo, F. Levi, and D. Calonico, "Absolute frequency measurement of the $^1S_0$–$^3P_0$ transition of ^{171}Yb," *Metrologia* **54**, 102–112 (2017).

25. A. D. Ludlow, M. M. Boyd, T. Zelevinsky, S. M. Foreman, S. Blatt, M. Notcutt, T. Ido, and J. Ye, "Systematic study of the ^{87}Sr clock transition in an optical lattice," *Phys. Rev. Lett.* **96**, 033003 (2006).

26. R. Le Targat, X. Baillard, M. Fouché, A. Brusch, O. Tcherbakoff, G. D. Rovera, and P. Lemonde, "Accurate optical lattice clock with ^{87}Sr atoms," *Phys. Rev. Lett.* **97**, 130801 (2006).

27. M. M. Boyd, A. D. Ludlow, S. Blatt, S. M. Foreman, T. Ido, T. Zelevinsky, and J. Ye, "^{87}Sr lattice clock with inaccuracy below 10^{-15}," *Phys. Rev. Lett.* **98**, 083002 (2007).

28. X. Baillard, M. Fouché, R. Le Targat, P. G. Westergaard, A. Lecallier, F. Chapelet, M. Abgrall, G. D. Rovera, P. Laurent, P. Rosenbusch, S. Bize, G. Santarelli, A. Clairon, P. Lemonde, G. Grosche, B. Lipphardt, and H. Schnatz, "An optical lattice clock with spin-polarized ^{87}Sr atoms," *Eur. Phys. J. D* **48**, 11–17 (2008).

29. G. K. Campbell, A. D. Ludlow, S. Blatt, J. W. Thomsen, M. J. Martin, M. H. G. De Miranda, T. Zelevinsky, M. M.

Boyd, and J. Ye, "The absolute frequency of the ^{87}Sr optical clock transition," *Metrologia* **45**, 539 (2008).

30. F.-L. Hong, M. Musha, M. Takamoto, H. Inaba, S. Yanagimachi, A. Takamizawa, K. Watabe, T. Ikegami, M. Imae, Y. Fujii, M. Amemiya, K. Nakagawa, K. Ueda, and H. Katori, "Measuring the frequency of a Sr optical lattice clock using a 120 km coherent optical transfer," *Opt. Lett.* **34**, 692 (2009).

31. S. T. Falke, H. Schnatz, J. S. R. V. Winfred, T. H. Middelmann, S. T. Vogt, S. Weyers, B. Lipphardt, G. Grosche, F. Riehle, U. Sterr, and C. H. Lisdat, "The ^{87}Sr optical frequency standard at PTB," *Metrologia* **48**, 399–407 (2011).

32. A. Yamaguchi, N. Shiga, S. Nagano, Y. Li, H. Ishijima, H. Hachisu, M. Kumagai, and T. Ido, "Stability transfer between two clock lasers operating at different wavelengths for absolute frequency measurement of clock transition in ^{87}Sr," *Appl. Phys. Express* **5**, 022701 (2012).

33. R. Le Targat, L. Lorini, Y. Le Coq, M. Zawada, J. Guéna, M. Abgrall, M. Gurov, P. Rosenbusch, D. G. Rovera, B. Nagórny, R. Gartman, P. G. Westergaard, M. E. Tobar, M. Lours, G. Santarelli, A. Clairon, S. Bize, P. Laurent, P. Lemonde, and J. Lodewyck, "Experimental realization of an optical second with strontium lattice clocks." *Nat. communications* **4**, 2109 (2013).

34. D. Akamatsu, H. Inaba, K. Hosaka, M. Yasuda, A. Onae, T. Suzuyama, M. Amemiya, and F.-L. Hong, "Spectroscopy and frequency measurement of the ^{87}Sr clock transition by laser linewidth transfer using an optical frequency comb," *Appl. Phys. Express* **7**, 012401 (2014).

35. S. Falke, N. Lemke, C. Grebing, B. Lipphardt, S. Weyers, V. Gerginov, N. Huntemann, C. Hagemann, A. Al-Masoudi, S. Häfner, S. Vogt, U. Sterr, and C. Lisdat, "A strontium lattice clock with 3×10^{-17} inaccuracy and its frequency," *New J. Phys.* **16**, 073023 (2014).

36. T. Tanabe, D. Akamatsu, T. Kobayashi, A. Takamizawa, S. Yanagimachi, T. Ikegami, T. Suzuyama, H. Inaba, S. Okubo, M. Yasuda, F. L. Hong, A. Onae, and K. Hosaka, "Improved Frequency Measurement of the $^1S_0 - ^3P_0$ Clock Transition in ^{87}Sr Using a Cs Fountain Clock as a Transfer Oscillator," *J. Phys. Soc. Jpn.* **84**, 115002 (2015).

37. Y.-G. Lin, Q. Wang, Y. Li, F. Meng, B.-K. Lin, E.-J. Zang, Z. Sun, F. Fang, T.-C. Li, and Z.-J. Fang, "First Evaluation and Frequency Measurement of the Strontium Optical Lattice Clock at NIM," *Chin. Phys. Lett.* **32**, 090601 (2015).

38. J. Lodewyck, S. Bilicki, E. Bookjans, J. L. Robyr, C. Shi, G. Vallet, R. Le Targat, D. Nicolodi, Y. Le Coq, J. Guéna, M. Abgrall, P. Rosenbusch, and S. Bize, "Optical to microwave clock frequency ratios with a nearly continuous strontium optical lattice clock," *Metrologia* **53**, 1123–1130 (2016).

39. C. Grebing, A. Al-Masoudi, S. Dörscher, S. Häfner, V. Gerginov, S. Weyers, B. Lipphardt, F. Riehle, U. Sterr, and C. Lisdat, "Realization of a timescale with an accurate optical lattice clock," *Optica* **3**, 563–569 (2016).

40. H. Hachisu, G. Petit, F. Nakagawa, Y. Hanado, and T. Ido, "SI-traceable measurement of an optical frequency at the low 10^{-16} level without a local primary standard," *Opt. Express* **25**, 8511–8523 (2017).

41. H. Hachisu, G. Petit, and T. Ido, "Absolute frequency measurement with uncertainty below 1×10^{-15} using International Atomic Time," *Appl. Phys. B* **123**, 34 (2017).

42. D. Akamatsu, M. Yasuda, H. Inaba, K. Hosaka, T. Tanabe, A. Onae, and F.-L. Hong, "Frequency ratio measurement of ^{171}Yb and ^{87}Sr optical lattice clocks," *Opt. Express* **22**, 7898 (2014).

43. M. Takamoto, I. Ushijima, M. Das, N. Nemitz, T. Ohkubo, K. Yamanaka, N. Ohmae, T. Takano, T. Akatsuka, A. Yamaguchi, and H. Katori, "Frequency ratios of Sr, Yb, and Hg based optical lattice clocks and their applications," *Comptes Rendus Physique* **16**, 489–498 (2015).

44. N. Nemitz, T. Ohkubo, M. Takamoto, I. Ushijima, M. Das, N. Ohmae, and H. Katori, "Frequency ratio of Yb and Sr clocks with 5×10^{-17} uncertainty at 150 seconds averaging time," *Nat. Photonics* **10**, 258–261 (2016).

45. J. Grotti, S. Koller, S. Vogt, S. Häfner, U. Sterr, C. Lisdat, H. Denker, C. Voigt, L. Timmen, A. Rolland, F. N. Baynes, H. S. Margolis, M. Zampaolo, P. Thoumany, M. Pizzocaro, B. Rauf, F. Bregolin, A. Tampellini, P. Barbieri, M. Zucco, G. A. Costanzo, C. Clivati, F. Levi, and D. Calonico, "Geodesy and metrology with a transportable optical clock," *Nat. Phys.* **14**, 437–441 (2018).

46. D. Akamatsu, T. Kobayashi, Y. Hisai, T. Tanabe, K. Hosaka, M. Yasuda, and F.-L. Hong, "Dual-Mode Operation of an Optical Lattice Clock Using Strontium and Ytterbium Atoms," *IEEE Transactions on Ultrason. Ferroelectr. Freq. Control.* **65**, 1069–1075 (2018).

47. M. Fujieda, S. Yang, T. Gotoh, S. Hwang, H. Hachisu, H. Kim, Y. Lee, R. Tabuchi, T. Ido, W. Lee, M. Heo, C. Y. Park, D. Yu, and G. Petit, "Advanced Satellite-based Frequency Transfer at the 10^{-16} Level," *IEEE Transactions on Ultrason. Ferroelectr. Freq. Control.* **65**, 973–978 (2018).

48. Y. B. Ovchinnikov, K. Szymaniec, and S. Edris, "Measurement of rubidium ground-state hyperfine transition frequency using atomic fountains," *Metrologia* **52**, 595–599 (2015).

49. J. Guéna, S. Weyers, M. Abgrall, C. Grebing, V. Gerginov, P. Rosenbusch, S. Bize, B. Lipphardt, H. Denker, N. Quintin, S. M. F. Raupach, D. Nicolodi, F. Stefani, N. Chiodo, S. Koke, A. Kuhl, F. Wiotte, F. Meynadier, E. Camisard, C. Chardonnet, Y. Le Coq, M. Lours, G. Santarelli, A. Amy-Klein, R. L. Targat, O. Lopez, P. E. Pottie, and G. Grosche, "First international comparison of fountain primary frequency standards via a long distance optical fiber link," *Metrologia* **54**, 348–354 (2017).

50. J. J. McFerran, L. Yi, S. Mejri, S. Di Manno, W. Zhang, J. Guéna, Y. Le Coq, and S. Bize, "Neutral atom frequency reference in the deep ultraviolet with fractional uncertainty = 5.7×10^{-15}," *Phys. Rev. Lett.* **108**, 183004 (2012).

51. R. Tyumenev, M. Favier, S. Bilicki, E. Bookjans, R. Le Targat, J. Lodewyck, D. Nicolodi, Y. Le Coq, M. Abgrall, J. Guéna, L. De Sarlo, and S. Bize, "Comparing a mercury optical lattice clock with microwave and optical frequency standards," *New J. Phys.* **18**, 113002 (2016).

52. K. Yamanaka, N. Ohmae, I. Ushijima, M. Takamoto, and H. Katori, "Frequency ratio of ^{199}Hg and ^{87}Sr optical

lattice clocks beyond the SI limit," *Phys. Rev. Lett.* **114**, 230801 (2015).

53. X. Baillard, M. Fouché, R. Le Targat, P. G. Westergaard, A. Lecallier, Y. Le Coq, G. D. Rovera, S. Bize, and P. Lemonde, "Accuracy evaluation of an optical lattice clock with bosonic atoms," *Opt. Lett.* **32**, 1812 (2007).

54. P. Morzynski, M. Bober, D. Bartoszek-Bober, J. Nawrocki, P. Krehlik, L. Sliwczynski, M. Lipinski, P. Maslowski, A. Cygan, P. Dunst, M. Garus, D. Lisak, J. Zachorowski, W. Gawlik, C. Radzewicz, R. Ciurylo, and M. Zawada, "Absolute measurement of the $^1S_0 - ^3P_0$ clock transition in neutral ^{88}Sr over the 330 km-long stabilized fibre optic link," *Sci. Reports* **5**, 17495 (2015).

55. H. Katori, M. Takamoto, T. Akatsuka, and H. Hachisu, "Optical lattice clocks with non-interacting bosons and fermions," *Nat. Phys.* **4**, 954–959 (2008).

56. T. Takano, R. Mizushima, and H. Katori, "Precise determination of the isotope shift of ^{88}Sr–^{87}Sr optical lattice clock by sharing perturbations," *Appl. Phys. Express* **10**, 089201 (2017).

57. M. S. Origlia, S.and Pramod, S. Schiller, Y. Singh, K. Bongs, R. Schwarz, A. Al-Masoudi, S. Dörscher, S. Herbers, S. Häfner, U. Sterr, and C. Lisdat, "A high-performance optical lattice clock based on bosonic atoms," (2018).

58. M. Chwalla, J. Benhelm, K. Kim, G. Kirchmair, T. Monz, M. Riebe, P. Schindler, A. S. Villar, W. Hänsel, C. F. Roos, R. Blatt, M. Abgrall, G. Santarelli, G. D. Rovera, and P. Laurent, "Absolute frequency measurement of the ^{40}Ca$^+$ $4s$ $^2S_{1/2} - 3d$ $^2D_{5/2}$ clock transition," *Phys. Rev. Lett.* **102**, 023002 (2009).

59. K. Matsubara, H. Hachisu, Y. Li, S. Nagano, C. Locke, A. Nogami, M. Kajita, K. Hayasaka, T. Ido, and M. Hosokawa, "Direct comparison of a Ca$^+$ single-ion clock against a Sr lattice clock to verify the absolute frequency measurement," *Opt. Express* **20**, 22034–22041 (2012).

60. Y. Huang, J. Cao, P. Liu, K. Liang, B. Ou, H. Guan, X. Huang, T. Li, and K. Gao, "Hertz-level measurement of the ^{40}Ca$^+$ $4s$ $^2S_{1/2} - 3d$ $^2D_{5/2}$ clock transition frequency with respect to the SI second through the Global Positioning System," *Phys. Rev. A* **85**, 030503 (2012).

61. Y. Huang, H. Guan, P. Liu, W. Bian, L. Ma, K. Liang, T. Li, and K. Gao, "Frequency comparison of two ^{40}Ca$^+$ optical clocks with an uncertainty at the 10^{-17} level," *Phys. Rev. Lett.* **116**, 013001 (2016).

62. C. Tamm, S. Weyers, B. Lipphardt, and E. Peik, "Stray-field-induced quadrupole shift and absolute frequency of the 688-THz ^{171}Yb$^+$ single-ion optical frequency standard," *Phys. Rev. A* **80**, 043403 (2009).

63. S. Webster, R. Godun, S. King, G. Huang, B. Walton, V. Tsatourian, H. Margolis, S. Lea, and P. Gill, "Frequency measurement of the Electric Quadrupole Transition in a Single ^{171}Yb$^+$ Ion," *IEEE Transactions on Ultrason. Ferroelectr. Freq. Control.* **57**, 592–599 (2010).

64. C. Tamm, N. Huntemann, B. Lipphardt, V. Gerginov, N. Nemitz, M. Kazda, S. Weyers, and E. Peik, "Cs-based optical frequency measurement using cross-linked optical and microwave oscillators," *Phys. Rev. A* **89**, 023820 (2014).

65. R. M. Godun, P. B. R. Nisbet-Jones, J. M. Jones, S. A. King, L. A. M. Johnson, H. S. Margolis, K. Szymaniec, S. N. Lea, K. Bongs, and P. Gill, "Frequency ratio of two optical clock transitions in ^{171}Yb$^+$ and constraints on the time variation of fundamental constants," *Phys. Rev. Lett.* **113**, 210801 (2014).

66. K. Hosaka, S. A. Webster, A. Stannard, B. R. Walton, H. S. Margolis, and P. Gill, "Frequency measurement of the $^2S_{1/2} - ^2F_{7/2}$ electric octupole transition in a single ^{171}Yb$^+$ ion," *Phys. Rev. A* **79**, 033403 (2009).

67. N. Huntemann, M. Okhapkin, B. Lipphardt, S. Weyers, C. Tamm, and E. Peik, "High-accuracy optical clock based on the octupole transition in ^{171}Yb$^+$," *Phys. Rev. Lett.* **108**, 090801 (2012).

68. S. A. King, R. M. Godun, S. A. Webster, H. S. Margolis, L. A. M. Johnson, K. Szymaniec, P. E. G. Baird, and P. Gill, "Absolute frequency measurement of the $^2S_{1/2}-^2F_{7/2}$ electric octupole transition in a single ion of ^{171}Yb$^+$ with 10^{-15} fractional uncertainty," *New J. Phys.* **14**, 013045 (2012).

69. N. Huntemann, B. Lipphardt, C. Tamm, V. Gerginov, S. Weyers, and E. Peik, "Improved limit on a temporal variation of m_p/m_e from comparisons of Yb$^+$ and Cs atomic clocks," *Phys. Rev. Lett.* **113**, 210802 (2014).

70. R. M. Godun, C. F. Baynham, J. M. Jones, S. A. King, P. B. Nisbet-Jones, F. Baynes, A. Rolland, P. E. Baird, K. Bongs, P. Gill, G. Petit, and H. S. Margolis, "Absolute frequency measurement of the ytterbium ion E3 optical clock transition using international atomic time," in *2018 European Frequency and Time Forum (EFTF),* (Turin, 2018), pp. 312–314.

71. T. Rosenband, P. O. Schmidt, D. B. Hume, W. M. Itano, T. M. Fortier, J. E. Stalnaker, K. Kim, S. A. Diddams, J. C. J. Koelemeij, J. C. Bergquist, and D. J. Wineland, "Observation of the $^1S_0 \rightarrow ^3P_0$ clock transition in ^{27}Al$^+$," *Phys. Rev. Lett.* **98**, 220801 (2007).

72. J. E. Stalnaker, S. A. Diddams, T. M. Fortier, K. Kim, L. Hollberg, J. C. Bergquist, W. M. Itano, M. J. Delany, L. Lorini, W. H. Oskay, T. P. Heavner, S. R. Jefferts, F. Levi, T. E. Parker, and J. Shirley, "Optical-to-microwave frequency comparison with fractional uncertainty of 10^{-15}," *Appl. Phys. B* **89**, 167–176 (2007).

73. T. Rosenband, D. B. Hume, P. O. Schmidt, C. W. Chou, A. Brusch, L. Lorini, W. H. Oskay, R. E. Drullinger, T. M. Fortier, J. E. Stalnaker, S. A. Diddams, W. C. Swann, N. R. Newbury, W. M. Itano, D. J. Wineland, and J. C. Bergquist, "Frequency ratio of Al$^+$ and Hg$^+$ single-ion optical clocks; metrology at the 17th decimal place," *Science* **319**, 1808–1812 (2008).

74. C. Degenhardt, H. Stoehr, C. Lisdat, G. Wilpers, H. Schnatz, B. Lipphardt, T. Nazarova, P. E. Pottie, U. Sterr, J. Helmcke, and F. Riehle, "Calcium optical frequency standard with ultracold atoms: Approaching 10^{-15} relative uncertainty," *Phys. Rev. A* **72**, 062111 (2005).

75. G. Wilpers, C. W. Oates, S. A. Diddams, A. Bartels, T. M. Fortier, W. H. Oskay, J. C. Bergquist, S. R. Jefferts, T. P. Heavner, T. E. Parker, and L. Hollberg, "Absolute frequency measurement of the neutral ^{40}Ca optical frequency standard at 657 nm based on microkelvin atoms," *Metrologia* **44**, 146–151 (2007).

76. K. R. Vogel, S. A. Diddams, C. W. Oates, E. A. Curtis, R. J. Rafac, W. M. Itano, J. C. Bergquist, R. W. Fox, W. D. Lee, J. S. Wells, and L. Hollberg, "Direct comparison of two cold-atom-based optical frequency standards by using a femtosecond-laser comb." *Opt. letters* **26**, 102–104 (2001).

77. V. A. Dzuba and V. V. Flambaum, "Limits on gravitational Einstein equivalence principle violation from monitoring atomic clock frequencies during a year," *Phys. Rev. D* **95**, 015019 (2017).